# Multi-MW Closed Cycle MHD Nuclear Space Power Via Nonequilibrium He/Xe Working Plasma

## Ron J. Litchford[1] and Nobuhiro Harada[2]

[1]*NASA Marshall Space Flight Center, Huntsville, AL 35812*
[2]*Nagaoka University of Technology, Nagaoka 940-2188, Japan*
*Contact: 256-544-1740; ron.litchford@nasa.gov*

**Abstract.** Prospects for a low specific mass multi-megawatt nuclear space power plant were examined assuming closed cycle coupling of a high-temperature fission reactor with magnetohydrodynamic (MHD) energy conversion and utilization of a nonequilibrium helium/xenon frozen inert plasma (FIP). Critical evaluation of performance attributes and specific mass characteristics was based on a comprehensive systems analysis assuming a reactor operating temperature of 1800 K for a range of subsystem mass properties. Total plant efficiency was expected to be 55.2% including plasma pre-ionization power, and the effects of compressor stage number, regenerator efficiency and radiation cooler temperature on plant efficiency were assessed. Optimal specific mass characteristics were found to be dependent on overall power plant scale with 3 $kg/kW_e$ being potentially achievable at a net electrical power output of 1-$MW_e$. This figure drops to less than 2 $kg/kW_e$ when power output exceeds 3 $MW_e$. Key technical issues include identification of effective methods for non-equilibrium pre-ionization and achievement of frozen inert plasma conditions within the MHD generator channel. A three-phase research and development strategy is proposed encompassing Phase-I Proof of Principle Experiments, a Phase-II Subscale Power Generation Experiment, and a Phase-III Closed-Loop Prototypical Laboratory Demonstration Test.

**Keywords:** Nuclear Space Power, Magnetohydrodynamic Energy Conversion, Nonequilibrium Plasma.

## INTRODUCTION

The principle technical obstacle to deep-space utilization of high-power nuclear electric propulsion (NEP) is the need for end-to-end system specific mass approaching 1 kg/kW. One of the few potentially feasible approaches for achieving the requisite power-to-weight performance are closed-cycle nuclear space power plants utilizing a High Temperature Gas Reactor (HTGR) coupled with a magnetohydrodynamic (MHD) generator, a concept readily scalable for application to multi-MW-class NEP systems. In contrast to turbo-generator systems, MHD generators extract energy at temperatures beyond solid material limits and provide high-temperature heat rejection. This advantage translates into weight savings via reduction in space radiator size and weight. If these potential specific power gains can be realized, it would open up entirely new vistas for rapid deep-space transport.

For many science-based robotic missions and surface power applications, power plant outputs of 100-120 $kW_e$ are considered readily achievable with currently available nuclear technologies, and various Advanced Radioisotope (AR) or Nuclear Fission Reactor (NFR) electric power generation systems could be engineered and developed with minimal R&D needs. For missions with larger electric power requirements, however, innovative low specific mass NFR systems with efficient electric power conversion are clearly needed. Here, we propose consideration of nuclear closed-cycle MHD (CCMHD) without bottoming cycle owing to the intrinsic high efficiency and compactness.
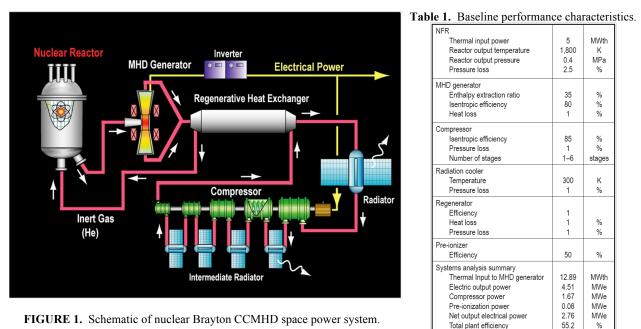
Thus far, thermoelectric converters (El-Genk and Saber, 2004; El-Genk and Tournier, 2004), stirling engines (Thieme and Schreiber, 2004), and turbo-brayton cycles (Zagarola *et al*., 2004; Godfroy *et al*., 2004) have been considered and studied as power conversion systems with AR power source for relatively smaller missions and with NFR for larger ones. For larger missions over 1 $MW_e$, gas-cooled NFR and vapor core reactors with CCMHD energy conversion have also been considered and studied (Litchford, *et al*., 2001; Knight and Anghaie, 2004).

Critical analysis of these advanced CCMHD concepts exhibit good potential for achieving low specific mass characteristics, but they typically require peak operating temperatures beyond currently available technology limits.

Here, we wish to examine an innovative CCMHD concept that can operate at less demanding reactor temperatures yet still approach the desired 1 kg/kW performance goal. In particular, we wish to consider Helium (He) and Xenon (Xe) frozen inert plasma (FIP) as an alternative to conventional alkali metal seeded fluids and to present the results of a concept study initiated at NASA-MSFC under the auspices of a visiting scientist cooperative agreement between the Japanese Ministry of Education and NASA HQ.

## INTEGRATED SYSTEM ARCHITECTURE

The integrated system architecture for the proposed NFR/CCMHD Brayton-cycle powerplant is illustrated in Fig. 1. Working medium of helium mixed with xenon is used so as to connect CCMHD system directly to the nuclear fission reactor. A He/Xe mixture is known to be an excellent coolant for gas-cooled reactors and is a good thermal insulator when stagnant (Wright *et al*., 2004). Moreover, the ionization characteristics of Xe are advantageous for generation of nonequilibrium plasma conditions, and it would avoid the difficult low temperature condensation problems associated with alkali metal seeded systems. In this concept, the bulk He carrier fluid is mixed with small amounts of Xe, which serves as the primary ionization seed. It is assumed that this inert gas mixture can be heated to no more than 1800 K in a solid core fission reactor due to practical constraints on fuel element temperature. Because the ionization potential of a Xe seeded working medium is much higher than conventional alkali-metal seeds (e.g., cesium), the natural ionization level, and therefore the electrical conductivity, are insufficient to invoke significant MHD interaction, and some form of electrical pre-ionization must be introduced at the entrance to the MHD generator for nonequilibrium plasma generation. Thus far, microwave, electron beam, helicon, and RF type systems have been identified and recommended as potentially viable candidates; however, the most suitable pre-ionization system will ultimately depend on subsystem effectiveness, reliability, simplicity, and specific mass characteristics as determined from laboratory evaluations and detailed design analyses. If the pre-ionization scheme can elevate the electron density and electron temperature sufficiently high and the effective recombination rate coefficient is sufficiently small, an FIP state can be established such that a high electron number density condition is sustained throughout passage through the MHD generator (Kobayashi and Okuno, 2000).



**FIGURE 1.** Schematic of nuclear Brayton CCMHD space power system.

**Table 1.** Baseline performance characteristics.

| NFR | | |
|---|---|---|
| Thermal input power | 5 | MWth |
| Reactor output temperature | 1,800 | K |
| Reactor output pressure | 0.4 | MPa |
| Pressure loss | 2.5 | % |
| MHD generator | | |
| Enthalpy extraction ratio | 35 | % |
| Isentropic efficiency | 80 | % |
| Heat loss | 1 | % |
| Compressor | | |
| Isentropic efficiency | 85 | % |
| Pressure loss | 1 | % |
| Number of stages | 1–6 | stages |
| Radiation cooler | | |
| Temperature | 300 | K |
| Pressure loss | 1 | % |
| Regenerator | | |
| Efficiency | 1 | |
| Heat loss | 1 | % |
| Pressure loss | 1 | % |
| Pre-ionizer | | |
| Efficiency | 50 | % |
| Systems analysis summary | | |
| Thermal Input to MHD generator | 12.89 | MWth |
| Electric output power | 4.51 | MWe |
| Compressor power | 1.67 | MWe |
| Pre-ionization power | 0.08 | MWe |
| Net output electrical power | 2.76 | MWe |
| Total plant efficiency | 55.2 | % |

The proposed system relies on a disk-shaped Hall-type MHD generator channel because of its simple, compact geometry with fewer electrode connections and because the basic design configuration is fundamentally compatibility with a simple split-coil superconducting magnet structure. The basic architecture incorporates a regenerative heat exchanger at the exhaust of the MHD channel in order to reclaim waste heat and improve plant

efficiency. Primary heat rejection occurs in a high-temperature radiator followed by staged compression using radiative inter-cooling. A portion of the direct current electrical power produced by the MHD generator is inverted and redirected to the compressors with the balance available for electric propulsion and/or spacecraft bus loads.

# ANALYSIS

Both a thermodynamic cycle analysis and comprehensive specific mass analysis were performed to estimate anticipated performance characteristics of the proposed powerplant system. Details and results of these analyses are summarized in the following subsections.

## Thermodynamic Cycle Analysis

Baseline thermodynamic cycle analysis results for the proposed nuclear Brayton CCMHD space power generation system are summarized in Table 1 and Fig. 2(a) assuming 5-MW thermal reactor power. In this case, we deduce a re-circulating regenerative power of about 8 MW implying 12.9 MW of thermal input power at the entrance to the MHD generator under steady state operating conditions. The total MHD electric power output is 4.51 MW of which 1.67 MW is consumed by the compressor bank and 0.08 MW is consumed by the pre-ionization system, yielding a net electric power output of 2.76 MW and an overall plant efficiency of 55.2 %. Achievable plant efficiency is primarily determined by the difference between the available gas temperature at the exit of the reactor and the heat rejection temperature in the radiators. We shall subsequently demonstrate, however, that design conditions for optimal plant efficiency do not correspond to those for optimal specific mass. In the proposed system, there are only three parametric design issues of major significance to cycle performance. These include compressor staging, regenerator effectiveness, and radiation cooler temperature.
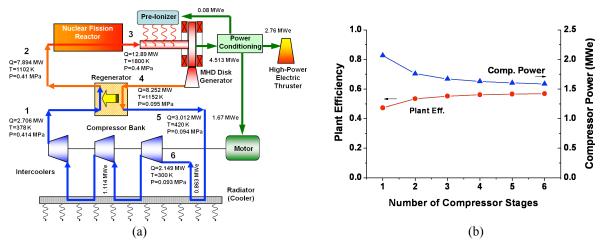


**FIGURE 2.** System performance characteristics: (a) thermodynamic state point summary; (b) compressor staging effects.

### Compressor Staging Effects

Variations in compressor power consumption and total plant efficiency versus number of compressor stages are shown in Fig. 2(b). It can be seen that plant efficiency increases with compressor stage number owing to increased number of intercoolers, which can reduce the power workload for pumping the working gas. Note, however, that the beneficial effect is not significant beyond three compressor stages.

### Regenerator Efficiency Effects

The temperature-entropy (T-s) diagram for the system is depicted in Fig. 3(a) for regenerator effectiveness (i.e. efficiency) of 1.0, 0.6, and 0.2. Here, the conditions at the exit of the reactor are set as the entropy reference point where both temperature and pressure are fixed. The cycle state points are delineated for the case of unity regenerator effectiveness where the working fluid gains thermal energy in the regenerator during process 1-2 and in the nuclear reactor during process 2-3. Processes 3-4 and 4-5 correspond to enthalpy extraction in the MHD

generator and in the regenerator, respectively. Process 5-6 represents radiative heat rejection followed by re-compression with inter-cooling between state points 6 and 1. Figure 3(b) depicts the re-circulating regenerative power, $Q_{REG}$, the thermal input power to the MHD generator, $Q_{MHD}$, and total plant efficiency, $\eta$, as a function of regenerator efficiency where the temperature difference between high- and low-temperature fluids is assumed to be 50 K.

Note that when regenerator efficiency is decreased and the amount of re-circulating regenerative heat is reduced, thermal input to the MHD generator must decrease if the reactor maintains a constant thermal output of 5 MW. Thus, decreased regenerative effectiveness decreases MHD generator electrical output and leads to a reduction in total plant efficiency. If the regenerator is completely removed from the system, plant efficiency decreases about 28%. If this lower level of plant efficiency is acceptable, then the regenerator can be removed from the system in order to reduce specific mass. However, to obtain the same level of electric power output as can be developed with fully regenerated heat, it is expected that the scale of the nuclear reactor, the MHD generator, and the radiation cooler would need to double. Thus, the optimal design configuration for attaining minimal system specific mass for a given electrical power output requires more detailed analysis comparisons.
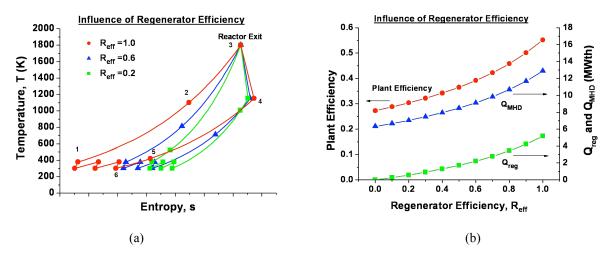


(a)                                                                                    (b)

**FIGURE 3.** Regenerator efficiency effects: (a) T-s diagram; (b) influence on powerplant efficiency.

### Radiator Temperature Effects

The T-s diagram of the system is depicted in Fig. 4(a) for radiation cooler temperatures of 300 K, 500 K, and 700 K. The cycle state points denoting the thermal power input processes and enthalpy extraction processes are identical for all radiation cooler temperatures. However, we clearly observe that total electric power generation, which corresponds to the area within the cycle diagram, increases significantly with decreasing radiator temperature. This implies that overall plant efficiency has a strong dependence on radiative cooling temperature. Figure 4(b), for instance, shows radiated waste heat, $Q_{RAD} = Q_{GC} + Q_{IC}$, and total plant efficiency versus radiator temperature. For space applications, waste heat must be entirely rejected via the radiative driving potential, which forces the radiator size and mass to increase rapidly as heat rejection temperature falls. Because the radiator temperature represents the bottoming temperature of the cycle, however, plant efficiency must fall dramatically as temperature rises. In this particular case, for instance, net electrical output power approaches zero when the radiative cooler temperature reaches 800 K. Because the radiated power exhibits a strong fourth-power dependence on radiator temperature, high-efficiency low-temperature operating characteristics require exceedingly large radiator sizes and mass. Thus, clarification of an optimal design strategy again requires careful analysis of system specific mass attributes.
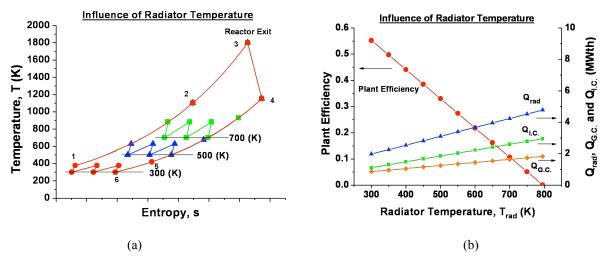
**FIGURE 4.** Radiator temperature effects: (a) T-s diagram; (b) influence on powerplant efficiency.

## Specific Mass Analysis

A general analysis of the systems specific mass characteristics is an extremely problematic undertaking in that the results tend to be highly sensitive to detailed point design features as well as subsystem and component technology assumptions. Here, we adopt the procedure, technology assumptions, and basic analysis strategy previously formulated by Litchford *et al*. (2001) in their landmark study of nuclear CCMHD space powerplant systems.

The resulting powerplant specific mass predictions are shown in Fig. 5 as a function of net electrical output power and radiator temperature. We observe that the specific mass decreases monotonically with increasing system power but, for a given specific power, a minimum value exists when the radiator temperature is around 600 K. To clarify why a minimum specific mass occurs at this particular value of the radiator temperature, it is useful to examine the mass fractions of major components, as shown in Fig. 6, for radiation cooler temperatures of 400 K, 600 K and 800 K. Note that as radiator temperature increases, the amount of area required to reject waste heat decreases substantially, and the radiator specific mass is reduced as expected. However, at the same time, larger MHD generator and superconducting magnet structures are required to provide the same net output power because total plant efficiency declines with the increases in the bottom cycle temperature. For instance, the mass of MHD generator and magnet at a radiator temperature of 800 K represents 36.4% of the total system mass, a value twice as large as observed when the radiator temperature drops to 600 K. On the other hand, the mass of the radiator itself grows rapidly with falling temperatures and accounts for more than 50% of total mass at radiator temperature of 300 K. Thus, there is a natural design minimum for a given power level requirement.
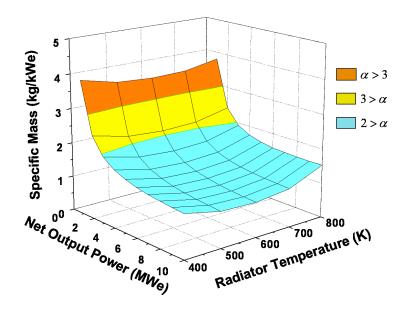


**FIGURE 5.** Estimated system specific power as a function of net electrical power output and bottom-side radiator temperature.

$$T_{rad} = 400\,\text{K}$$
$$\alpha = 1.28$$

$$T_{rad} = 600\,\text{K}$$
$$\alpha = 1.01$$

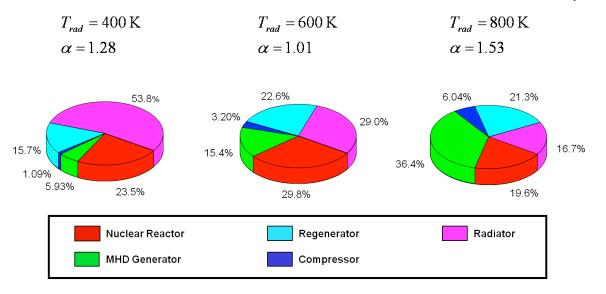$$T_{rad} = 800\,\text{K}$$
$$\alpha = 1.53$$

**FIGURE 6.** Major component mass fractions for radiator temperatures of 400 K, 600 K, and 800 K.

If we choose the appropriate minimizing radiator temperature in this case, we estimate a specific mass range of about 3 kg/kW$_e$ for 1 MW$_e$ of output power, 2~3 kg/kW$_e$ for 2 MWe of output power, and less than 2 kg/kW$_e$ for the net electrical outputs larger than 3 MW$_e$. We therefore conclude that the proposed nuclear CCMHD power generation system should provide both higher plant efficiency and much lower specific mass for a given level of electrical output power compared with other energy conversion systems, provided that the targeted performance and mass characteristics are achievable.

## RESEARCH & DEVELOPMENT PLAN

The positive analysis results for the proposed nuclear CCMHD power generation system are suggestive of promising system characteristics, but practical verification and confirmation will require an orderly and logical sequence of research and development. Based on careful consideration of the challenges and significant technical concerns, we would suggest the following three-phase research and development plan to include; Phase-I: Proof of Principle, Phase-II: Subscale Power Generation, and Phase-III: Prototypical Closed Loop System Demonstration.

## Phase I: Proof of Principle

Performance of a CCMHD generator using helium and xenon mixture as working medium depends on ionization and recombination processes. For example, stable operation in the regime of fully ionized Xe seed against ionization instability cannot be expected because the critical Hall parameter is reduced below levels available with alkali metal seed. However, previous computational studies have shown that nonequilibrium He-Xe plasmas can be temporarily stabilized in the MHD generator with high performance characteristics if the characteristic time for recombination is long enough compared with the residence time (Harada and Tashiro, 2003). Therefore, it is suggested that the initial phase of R&D should concentrate on basic plasma physics issues and clarification on whether the pre-ionization level (i.e., electron number density and electrical conductivity) can be sustained and stabilized over a time interval long enough to accommodate passage through a disk MHD channel, where the electron number density and temperature are initially elevated well above the equilibrium level via electrical pre-ionization methods. The primary technical objective would be to demonstrate that, if the characteristic time for recombination is much longer than the required residence time of the plasma, the process becomes "frozen" and the initial ionization level can be kept high. In this case, the plasma is pseudo-stable and high generator performance can be achieved without the use of condensable alkali-metal seed.

The basic schematic for a suggested laboratory proof of principle experiment is shown in Fig. 7(a) where a He/Xe gas mixture is pre-ionized in a plenum by various possible methods such as radio-frequency, microwave, helicon, or electron beam induced ionization. Time variations in ionization conditions could then be monitored through measurements of electron number density and electrical conductivity. A total mass flow rate of 0.16 kg/s is utilized to match the conditions deemed appropriate for a Phase II subscale power generation demonstration. In order to achieve an ionization degree of $10^{-4} \sim 10^{-6}$, pre-ionization power is estimated to be about 3 kW$_e$ assuming a pre-ionizer efficiency of 50%. An acceleration nozzle is incorporated between the pre-ionization chamber and the test section to simulate an MHD channel. In the test section, changes in electron number density and electrical conductivity along the flow direction could be measured using microwave cut-off, attenuation, and phase shift. It is anticipated that the total duration of an experiment would not exceed tens of seconds depending on measurement requirements. Detailed operating conditions are summarized in Table 2.

## Phase II: Subscale Power Generation

Phase II follow-on activity would focus on the execution of subscale power generation demonstrations to verify performance and operational characteristics. A basic schematic of the Phase II experiment is shown in Fig. 7(b), where scale and operating parameter ranges are governed by both cost and research and development requirements. A He/Xe working gas mixture is first heated to 1,800 K, the expected exit temperature of an NFR, using an electric heater and an existing 1.5-MWe arc-heater at NASA MSFC. The gas exit temperature of the vapor core reactor is considered to be in that range while the exit temperature of a direct-drive gas-cooled reactor would be around 900 to 1,150 K. Next, pre-ionized working gas is introduced to the disk MHD generator, and a magnetic field is applied using a 3-T split-coil superconducting magnet. Because a high Hall parameter must be maintained in the disk generator channel, the stagnation pressure should be ≈0.2 MPa at this magnetic field strength with a Mach number of around 2 to 2.5 at the disk channel inlet. For the pin-type gas-cooled reactor, the operating pressure is ≈2.4 MPa. Thus, the optimum design of an MHD generator and operating conditions for lower temperature and higher gas pressure should also be studied. In this Phase II configuration, the exit of the generator should be connected to an ejector in order to maintain low backpressure on the device.

To obtain the specified thermal input, the He/Xe mixture would be preheated to 1,050 K using an electric heater with additional heat provided by an arc-heater to raise the temperature to 1,800 K; therefore, the total thermal input to the working fluid would be 1.5-MWth. This thermal input is comparable to the He shock tube experiments at T.I.T., which has demonstrated enthalpy extraction ratios >30%. Stagnation gas temperature must be close to the exit temperature of an NFR, which was set at 1,800 K. The required net electric power for pre-ionization of Xe, up to an ionization degree of $10^{-4}$ to $10^{-6}$, is ≈4.7 kWe, and pre-ionizer power must be ≈10 kWe if ionization efficiency is assumed to be ≈50%. The proposed operating conditions and results of the preliminary MHD generator design are summarized in Table 3. The resulting MHD channel-shape design is depicted in Fig. 8(a). Inlet and exit radii are 0.05 m and 0.2 m, respectively. Channel height is <0.02 m and total disk height, including thermal insulator and support structure, is expected to be <0.1 m. This disk channel design would therefore fit within NASA MSFC's existing 3-T split-coil superconducting magnet, and operation with a higher magnetic field, if available, could reduce the warm gap from 12 to 5 in. Figure 8(b) summarizes predicted plasma parameter distributions for the proposed baseline MHD disk design.
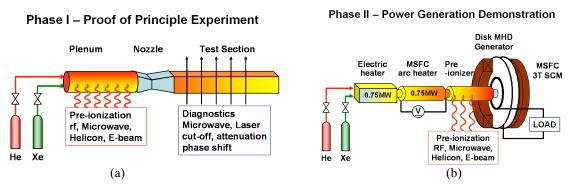


**Phase I – Proof of Principle Experiment**

**Phase II – Power Generation Demonstration**

(a)

(b)

**FIGURE 7.** Proposed experiment schematics: (a) proof of principle; (b) subscale power generation demonstration.

For the proposed Phase II subscale power generation experiment configuration, it should be possible to demonstrate >20% enthalpy extraction. In the previous system analysis, an enthalpy extraction of 35 percent and isentropic efficiency of 80 percent have been assumed. This level of performance can be confirmed through numerical simulations if the magnetic field strength is increased to 8 T.

**Table 2.** Phase I experiment parameters.

| Location | M | T (K) | p (MPa) | u (m/s) | A (cm²) |
|---|---|---|---|---|---|
| Pre-ionizer | 0.3 | 291 | 0.186 | 301 | 17.3 |
| Test section | 1 | 225 | 0.097 | 883 | 8.7 |

Plenum Stagnation Conditions: $T_0$=300 K, $P_0$=0.2 MPa.

**Table 3.** Phase II experiment parameters.

| Baseline operating conditions | | |
|---|---|---|
| Working fluid | He/Xe (seed) | |
| Thermal input power | 1.5 | MWth |
| Stagnation temperature | 1,800 | K |
| Stagnation pressure | 0.2 | MPa |
| Mass flow rate | 0.16 | kg/s |
| Seed fraction | $10^{-5}$–$10^{-4}$ | |
| Pre-ionization power | 4.7 | kWe (net) |
| MHD disk generator design summary | | |
| Inlet radius | 5 | cm |
| Exit radius | 20 | cm |
| Inlet height | 1.5 | cm |
| Exit height | 1.1 | cm |
| Inlet Mach number | 2 | |
| Exit Mach number | 0.64 | |
| Inlet radial velocity | 2,310 | m/s |
| Exit radial velocity | 1,340 | m/s |
| Output current | 122.4 | A |
| Output voltage | 2,905 | V |
| Output electrical power | 0.356 | MWe |
| Enthalpy extraction ratio | 23.7 | % |

## Phase III: Prototypical Closed-Loop System Demonstration

From a long-term perspective, Phase III efforts would be devoted to the construction of a complete closed loop system with a simulated non-nuclear heat source and the conduct of continuous power generation tests to confirm generator performance characteristics. The main technical objectives would be to confirm closed-loop system performance and stability, start-up and shutdown operations, output controllability, system reliability, and durability. Ultimately, the CCMHD system should be connected to an actual fission reactor in a full-up ground test demonstration experiment.
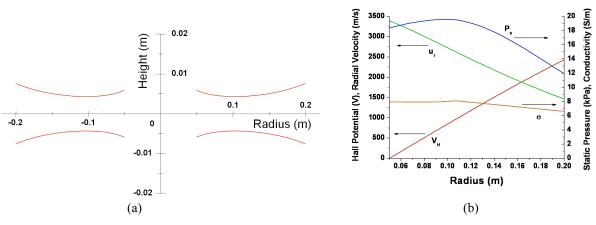


**FIGURE 8.** Phase II subscale design characteristics: (a) MHD channel lofting; (b) predicted plasma parameter distributions.

## CONCLUSIONS AND RECOMMENDATIONS

A concept for multi-megawatt nuclear CCMHD space power plant cycle using nonequilibrium He/Xe working plasma has been suggested as a promising basis for achieving low specific mass space exploration systems, and preliminary technical evaluations have been completed with positive indications. The evaluation studies included detailed thermodynamic and system specific mass analyses along with the formation of a comprehensive R&D plan aimed at technical feasibility demonstration, development of critical enabling technologies, and breadboard system demonstrations that would advance technical readiness to a level that would support the initiation of a flight demonstration program.

# ACKNOWLEDGMENTS

# REFERENCES

EL-GENK, M.S. and SABER, H.H., "Cascade Thermoelectric Converters-Advanced Radioisotope Power Systems (CTC-ARPSs)," *Space Technology and Applications International Forum (STAIF) 2004*, *AIP Proceedings 699*, pp. 230-241, (2004).

EL-GENK, M.S. and TOURNIER, J-M., "Conceptual Design of HP-STMCs Space Reactor Power System for 110kWe," *Space Technology and Applications International Forum (STAIF) 2004*, *AIP Proceedings 699*, pp. 658-672 (2004).

GODFROY, T.J., KAPERNICK, R.J. and BRAGG-SITTON, S.M., "Thermally Simulated 32kW Direct Drive Gas Cooled Reactor: Design, Assembly, and Test," *Space Technology and Applications International Forum (STAIF) 2004*, *AIP Proceedings 699*, pp. 757-763 (2004).

HARADA, N. and TASHIRO, T., "Influence of Recombination Coefficient on Discharge Structure and Plasma Stability in Closed Cycle MHD Generator with He/Xe Working Gas," AIAA-2003-3762 (2003).

KNIGHT, T. and ANGHAIE, S., "Estimation of Specific Mass for Multimegawatt NEP Systems Based on Vapor Core Reactors with MHD Power," *Space Technology and Applications International Forum (STAIF) 2004*, *AIP Proceedings 699*, pp. 379-387 (2004).

KOBAYASHI, H. and OKUNO, Y., "Feasibility Study on Frozen Inert Gas Plasma MHD Generator," *IEEE Transactions on Plasma Science*, Vol. 28, No. 4, pp. 1296-1302 (2000).

KOPPEL, C.R., VALENTIAN, D., LATHAM, P., FEARN, D., BRUNO, C., NICOLINI, D., ROUX, J.P., PAGANUCCI, F., and SAVERDI, M., "Preliminary Comparison Between Nuclear-Electric and Solar-Electric propulsion Systems for Future Mars Missions," *Space Technology and Applications International Forum (STAIF) 2004*, *AIP Proceedings 699*, pp. 369-378 (2004).

LITCHFORD, R.J., BITTEKER, L.J. and JONES, J.E., "Prospects For Nuclear Electric Propulsion Using Closed-Cycle Magnetohydrodynamic Energy Conversion," *NASA/TP-2001-211274* (2001).

THIEME, L.G. and SCHREIBER, J.G., "Advanced Technology Development for Stirling Converters," *Space Technology and Applications International Forum (STAIF) 2004*, *AIP Proceedings 699*, pp. 432-439 (2004).

WRIGHT, S.A., LAPINSKI, R.J., GODFROY, T.J., BRAGG-SITTON, S.M., and VAN DYKE, M.K., "Direct-Drive Gas-Cooled Reactor Power System: Concept and Preliminary Testing," *Space Technology and Applications International Forum (STAIF) 2003*, *AIP Proceedings 654*, pp. 445-450 (2004).

ZAGAROLA, M.V., CROWLEY, C.J., and SWIFT, W.L., "Progress on Low-Power Turbo-Brayton Converters," *Space Technology and Applications International Forum (STAIF) 2004*, *AIP Proceedings 699*, pp. 453-462 (2004).